Changes in damaging hail in major Australian cities with global warming

Timothy H. Raupach[1,2,3], Joanna Aldridge[4,5]

[1]UNSW Institute for Climate Risk and Response, UNSW Sydney, New South Wales, Australia
[2]UNSW Climate Change Research Centre, UNSW Sydney, New South Wales, Australia
[3]ARC Centre of Excellence for Climate Extremes, Sydney, New South Wales, Australia
[4]School of Geosciences, University of Sydney, Sydney, New South Wales, Australia
[5]QBE Australia, Sydney, New South Wales, Australia

Key Points:

- Hail causes more damage when hailstones are larger or coincident winds are stronger, yet there is high uncertainty in the changes in these factors with global warming.
- Convection-permitting downscaled simulations were used to investigate possible future changes in hail size and coincident wind strength over major Australian cities and the remote Western Australian Goldfields region. **(JA: state scenario and timeframe)**
- The projections indicate increases in hailstorm severity in areas around the major population centers of Melbourne, Canberra and Sydney, with increased windblown hail risk in the remote Goldfields region, and non-significant changes in other studied domains. **(JA: confusing, doesn't say same thing as abstract)**

Corresponding author: Timothy H. Raupach, `timothy.h.raupach@gmail.com`

Abstract

In Australia, hailstorms are a leading cause of insured losses, with damage exacerbated if hailstones are larger or there are coincident strong winds. Despite the high damage potential of such storms, changes to their frequency and severity under global warming are not well understood. Here, we use downscaled simulations over major cities and a remote region in Australia to project changes in hail frequency, hailstone size, and coincident wind speeds under a future scenario with ∼2.8 ° Celsius warming over pre-industrial global mean temperature. The study regions cover over 60% of the total Australian population. Generalized extreme value analysis was used to examine changes in daily maximum hail sizes and coincident wind speeds. The projections show higher future hail damage potential in some regions, with increases in hail frequency in the Sydney/Canberra and Brisbane regions, and robust increases in maximum hail size and coincident wind strength in the Melbourne and Sydney/Canberra regions.

Plain Language Summary

Hailstorms endanger lives and damage property, leading to large insurance losses in Australia. Hailstorms are more damaging if the hailstones they produce are larger. They are also more damaging if there is high wind at the same time, because the wind can push hailstones sideways into breakable materials such as windows or house facades. We expect climate change to affect hailstorms, but there have been few studies on how hailstorm frequency and severity may change in future in Australia. In this study we used simulations of weather in a future, warmer climate scenario to look at possible changes in hailstone size and in the strength of winds when hail occurs, over major cities and a remote area in Australia. The simulations project an increase in hail severity for the heavily populated Melbourne and Sydney/Canberra regions, an increase in hail frequency in Sydney/Canberra and Brisbane regions, and no significant changes in the other areas we studied.

1 Introduction

Hailstorms are most damaging when the hailstones they produce are larger (Brimelow et al., 2002; Eccel et al., 2012), and when there are coincident strong winds that push hailstones laterally (Changnon, 1967; Towery et al., 1976). While anthropogenic climate change is expected to affect severe convective storms (Allen, 2018) and their associated hazards of hail (Raupach et al., 2021) and extreme winds (Brown & Dowdy, 2021), there remains high uncertainty and geographical heterogeneity in projections of how these changes may manifest (Raupach et al., 2021; Brown & Dowdy, 2021), and changes in the coincidence of hail and high winds have been virtually unstudied. Here, we use high-resolution downscaled simulations of a future, warmer environment to compare changes in hail damage potential over hail-prone areas of Australia. **(JA: suggest a bit more about the study aims/framework as this is useful for the reader to understand upfront – ie one climate scenario, one time frame, CMIP6 ensemble)**

(Impacts in Australia) Severe convective storms are responsible for insured losses of over $A40b in Australia from 1967 to 2023 (in 2022 dollars), accounting for 25% of insured catastrophe losses (Insurance Council of Australia, 2024). The largest insured loss for any catastrophe event in Australian history, at $A8.845b (normalized to 2022 dollars, Insurance Council of Australia, 2024), was caused by the April 1999 hailstorm impacting the eastern suburbs of Sydney. Canberra and Brisbane have also experienced hail events with normalized losses over $A1b (Insurance Council of Australia, 2024) **(check ref)**.

(Reasons for combining hail and wind) Hail and convective winds are often studied separately, with typical severe convective storm catastrophe models generating synthetic event sets of hail and wind hazards as separate event footprints **(ref)**. However, the coincidence of wind and hail is an important driver of loss. Wind-driven hail, both due to its

greater force and oblique angle of impact, has greater potential to injure people, destroy crops (Changnon, 1967; Towery et al., 1976) and cause damage to the built environment, such as damaging cladding to external walls, breaking windows of buildings and motor vehicles and letting rainwater inside to damage internal fixtures and contents **(ref)**. Examination of recent high-loss hail events in Australia shows that wind is often mentioned as a contributing factor **(ref)**. Common thresholds for damaging conditions include hail over 2 cm in diameter **(ref)** or wind gusts over 90 km h^{-1} (Allen, 2018). Wind driven hail events are defined here as hail exceeding 5 cm in diameter and wind gusts exceeding 100 km/h (27.8 m/s) occurring in the same system within a one-hour timeframe **(ref)**. Wind driven hail events are most likely to be associated with supercells where downbursts occur **(ref)**. Observational data in the United States of America (USA) identified squall lines, isolated cells, and clusters of cells as the most frequent systems associated with wind driven hail (Carletta, 2010). (Bell et al., 2023) compiled 1646 hail and wind damage swaths for the mid-west of the USA using satellite observations for use in future understanding of the frequency of these events. No such studies for Australia have been identified.

(What is known of hail and wind changes with global warming) (Allen et al., 2014) used an environment-based approach to suggest an increase in severe thunderstorm incidence in south-east Australia, although with a wide range of uncertainty. (Walsh et al., 2016) review the current and future storm-related wind and hail hazard in Australia and found future projections of wind hazard increase along the populated east coast of Australia. **(More to add here. JA: You need to add your own studies – I suggest we could move this to be Para 2 in the introduction?)**

(JA's text re case study events) A selection of recent large loss causing hail events in Australia associated with both giant hail and strong winds include:

- October 2020 "Hailoween" hail storm impacting the southern suburbs of Brisbane;
- January 2020 "Tri City" hail storm impacting Canberra, Melbourne and Sydney;
- April 2020 Rockhampton hail storm impacting the Queensland towns of Rockhampton and Yeppoon.

These three case studies are described in more detail below.

(JA: To Add: Coloured charts? I don't have any that aren't proprietary. JA provided black and white synoptic charts in word document.)

(Hailoween) The October 2020 'Hailoween' hail storm generated a series of at least nine super cells in a corridor from Amberley to Logan that generated giant hail stones reported as 7 cm in Gympie, giant hail up to 14 cm at Forestdale, 13cm at Hillcrest, 9.5 cm at Amberley, 8 cm at Springfield, 7 cm at Gatton, and 5 cm at Seventeen Mile Rocks. The hardest hit suburbs were Singfield, Springfield Lakes, Rosewood, Thagoona and Willowbank. Strong winds were also recorded, with 100 kmh 3-second gusts occurring around Moreton Bay and wind damage evident from Redcliffe to Kingston. The State Emergency Service received 2900 call outs and power outages affected 95 000 people. The storms were associated with a series of complex fronts and embedded lows in the monsoon inland trough, following a week of instability over eastern Australia (Figure X). The Queensland Reconstruction Authority (QRA)'s initial assessment immediately after the hailstorm identified 520 properties with severe damage, 602 dwellings with moderate damage and 652 properties with minor damage. Extensive damage was reported to roofs, skylights, solar panels, interior, awnings, windows, shutters, ceiling collapse, falling trees. Water ingress following hail damage was widespread, leading to damage to interior walls and floors, mould, and contents damage. Some houses experienced hail damage through the roofs, solar panels and interior ceiling into the living areas of the home. This event resulted in an insured loss of $A1.056b from around 44,700 claims **((Insurance Council of Australia,**

2024)). (Reference: https://knowledge.aidr.org.au/resources/hailstorm-south-east-queensland-2020/)

(Tri-city storm) The 20th January 2020 "Tri-City" storms impacted a wide area of eastern Australia immediately following the devastating "Black Summer" bushfires. The storms impacted three major cities: Canberra, Sydney and Melbourne as well as country NSW areas of Queanbeyan and Goulburn. Canberra received 5–7 cm hail impacting the Central Business District and densely populated inner suburbs including the Australian National University. A 117 km h wind gust was recorded at Canberra Airport. Melbourne received hail of up to 5.5 cm over the southeastern suburbs along with damaging winds, heavy rainfall and flash flooding. Sydney received up to 7 cm hail over the outer southern suburbs of Campbelltown and the Sutherland Shire. The meteorological situation showed an inland trough extending from central Queensland through southeastern Australia, with an upper level low and associated surface level low creating moist unstable air. The extensive damage in Canberra included broken windows and sky lights in homes and commercial buildings, flooding, and thousands of cars damaged by hailstones. Wind damage includes fallen trees, branches and power lines, and blocked roads. There was structural damage to buildings at the Australian National University and civil buildings in the central business district. This event resulted in around 132 000 claims and a $A1.68b insured loss ((Insurance Council of Australia, 2024)). (Reference: https://knowledge.aidr.org.au/resources/hailstorms-and-heavy-rainfall-victoria-january-2020/)

(Rockhampton) The April 2020 hailstorm impacted the central Queensland towns of Rockhampton and Yeppoon and surrounding areas located on the Tropic of Capricorn. The weather pattern was due to an upper-level trough crossing central Queensland combined with a surface trough. Storm activity propagated from inland moving northeast to the coast, with a large supercell impacting the corridor from Rockhampton to Yeppoon. Giant hail of 8 to 12 cm was reported as well as 100 kmh 3-second wind gusts. Damage included holes in roofs, smashed windows and car windscreens, some flooding and tree damage. The timing of this event during the first Covid lockdown complicated recovery efforts. An insured loss of $A503m from around 15 000 claims was incurred (Insurance Council of Australia, 2024). In the Whitsunday region, golf ball size hail was reported in Sarina. The time of year, size of hail and the tropical latitude of this event made it highly unusual. (References: https://www.swissre.com/australia_newzealand/insights/rockhampton--hail.html https://www.earlywarningnetwork.com.au/news/record-hailstorms-lash-central-queensland https://www.abc.net.au/news/2020-04-20/supercell-storm-causes-widespread-damage-in-central-queensland/12163780)

(Australian context re building codes) While wind loadings are currently considered in the Australian building code (Australian Building Codes Board, 2024) under standard AS1170.2 (Standards Australia, 2021), the impact of hail and wind-driven hail is not currently considered in Australian building design. The Association of Consulting Structural Engineers (2022) discuss hail loading on roofs and acknowledge that this effect is not accounted for under the current design standards. The April 2015 hail event impacting western Sydney is discussed including the collapse of warehouse buildings from hail loading on roofs. A guide of ultimate limit and service limit state designs for various building types is presented, but wind driven hail is not considered. Some roofing products are tested for hail impacts against standards, but many products are unrated. In the ICC building code (International Code Council, 2008), hail is considered in two hail regions in the USA defined using observational data: moderate and severe, depending on the likelihood of at least one day of 1.5–3 mm (check) hail in a 20-year period. This code requires testing of roofing materials such as asphalt, wood and slate shingle, clay or concrete tiles, metal roofing panels and shingles in these zones. The changing occurrence of hail over time is not considered in that code. In Canada, while hail impact is not considered in the current building code, change is being sought in the aftermath of the 2020 Calgary hailstorm which caused $C1.4b of insured loss. Resilience measures may include increasing roof slope, using

resistant roofing materials and roof underlays (Institute for Catastrophic Loss Reduction, 2018). A finding was that a steeper roof limits damage from wind-driven hail on the leeward side of a property. The lack of research into impact resistant non-roof housing elements, such as windows, doors, sidings, fascia and skylights, is noted, and these elements are often subject to damage in the most destructive storms.

(What we have done here) Here, we seek to understand how the coincidence of extreme winds and damaging hail may change in a future climate in Australia. We conducted analyses covering the major Australian cities of Perth, Adelaide, Melbourne, Canberra, Sydney, and Brisbane, and a remote region around the town of Kalgoorlie in the Western Australian Goldfields. The populations of these cities covers over 60% of the total Australian population **(ref)**. Proxy-based climatologies show these regions to be hail-prone (Raupach, Soderholm, Warren, & Sherwood, 2023).

(JA: mention additional results that are presented in the results section and why we ar e considering these ie regional correlations in hail trends, changes in convective parameters. "We investigate regional correlations in hail trends both directly from the hail size datasets and indirectly via the trends in convective parameters, in order to better understand the potential for growth in hail hazard in the domains surrounding Australia's major population centres. Growing risk in multiple locations may present a challenge to community resilience and the insurance industry by requiring more robustness and redundancy in both the supply chain and capital to repair damage across several states. Understanding the trends in the contributing convective parameters aids our understanding of the driving processes behind projected hail changes.")

2 Methods

2.1 Simulations of historical and projected weather

Historical and future simulations were produced using the Advanced Research Weather Research and Forecasting (AR-WRF) weather model version 4.4.1 (Skamarock et al., 2021) for six nested domains. Two model configurations were used, with settings other than the domain configurations the same for both (Supporting Information Table S1). In total, we used two coarse- (∼27 km grid spacing), four medium- (∼9 km), and six fine-resolution (∼3 km) domains with a parent-child scaling ratio of three (Supporting Information Figure S1). WRF-HAILCAST (Adams-Selin et al., 2019) was enabled for the fine-resolution domains, to estimate maximum hailstone diameters at the surface. Boundary condition inputs were prepared using the `nc2wrf` code of Xu et al. (2021a).

Simulations were run for two epochs of 20 convective seasons each: the historical epoch ran from 1989 to 2009, and the future epoch from 2080 to 2100. For each convective season, simulations were run from 00Z September 30 to 18Z February 28, with hourly output resolution. Outputs were converted to local summer time and subset to cover October 1 to February 28 inclusive in each season. For each season the 14 to 16 simulated hours on 30 September local time were discarded as model spin-up time. Model outputs provide instantaneous hourly values for most variables, including wind speed at 10 m **(JA: above ground level?)**. In contrast, for each grid point and each hour, HAILCAST output the maximum hail diameter over all model time steps during the previous hour. The time step for the coarse domain was set to 100 s, but reduced to 80 s or 60 s for simulation days on which Courant-Friedrichs-Lewy (CFL) errors occurred. HAILCAST was run at every model time step, so on those days for which the time step was reduced, HAILCAST ran more often. However, here we use maximum hail sizes per day, and the sample of hail sizes per day is large, so we expect minimal effect of this time step variability. Except for the overall maxima shown in Section 4.1, we subset all our analyses to consider only times and locations where there was non-zero surface hail recorded in the preceding hour. Wind

speeds and convective parameters are thus instantaneous values in temporal proximity to hail occurrences.

2.2 Processing of simulation outputs

Examination of maximum hail size fields showed that HAILCAST occasionally produced unreasonably large hail sizes, particularly over water bodies (Supporting Information Figure S2). Since our focus is on hail hazard on land, we subset the data to land areas using the WRF land mask with small holes filled and a slight erosion applied so that points over the ocean, large bodies of water, or directly over the coastal boundary are not considered in this study. Further, we removed from consideration any HAILCAST value of surface hail over 180 mm diameter (this value being greater than the largest hail ever observed in Australia, at ∼16 cm, Australian Bureau of Meteorology, 2021) **(JA: discarding HAILCAST outputs ¿18 cm – would it be more reasonable to cap it then discard this data?)**. HAILCAST has been updated in more recent versions of WRF than used here, and while the updated version reduces the occurrence of unrealistically large hail sizes the changes do not affect the majority of HAILCAST results, meaning that removing very large hail sizes, as we do here, leaves a reasonable dataset for analysis (pers. comm. B. Adams-Selin, 2024). In all, less than 0.006% of non-zero hail-diameter values (not over water) were removed for being too large, per domain. Convective parameters were calculated as described in Raupach, Soderholm, Protat, and Sherwood (2023). **(JA: Suggest mentioning what the parameters are and maybe a brief description.)**

2.3 Statistical modelling of extreme values

Extreme value analysis was completed using the R (R Core Team, 2023) package `extRemes` (Gilleland & Katz, 2016). Block maxima were defined as daily maximum hailstone sizes and wind speeds at hail locations per domain, under the assumption that such time series can be considered independent (Coles, 2001) because single hail storms do not last more than one day. Generalized extreme value (GEV) distributions were fitted to each series of block maxima. We used quantile-quantile (QQ) plots (Coles, 2001) and the Kolmogorov–Smirnoff (KS) test to assess the goodness of fit of the GEV distributions, by examining the similarity of the empirical distributions of block maxima and values drawn from the fitted GEV distributions. The KS test was also used to examine the (dis)similarity of GEV distributions fitted to historical versus future epochs. When the KS test was used, we generated a probabilistic view of the similarity between distributions by drawing 1000 values from the GEV distribution(s), applying the KS test, and repeating this process 100 times to generate 100 KS test results. **(JA: suggest moving the EV section below the Data Section.)**

3 Data

Boundary conditions used for the simulations were bias-corrected data for downscaling by Xu et al. (2021b). These boundary conditions have a mean climate and interannual variance derived from European Centre for Medium-Range Weather Forecasts Reanalysis 5 (ERA5, Hersbach et al., 2020), with a non-linear trend derived from the ensemble mean of 18 Coupled Model Intercomparison Project Phase 6 (CMIP6, Eyring et al., 2016) models (Xu et al., 2021b). Future projections used the "middle-of-the-road" SSP2-4.5 shared socioeconomic pathway (SSP, O'Neill et al., 2017). On average the historical period in our simulations (1989–2019) had a global mean temperature 0.39 K above pre-industrial temperatures (1850–1990, using the CMIP6 35-model ensemble, Gutiérrez et al., 2021) while the future period (2080–2099) had a global mean temperature 2.81 K over pre-industrial temperatures. The historical and future epochs were thus separated by 2.42 K of warming.

4 Results

4.1 Overall maxima

Before taking a more rigorous statistical approach, it is useful to consider the maps of overall maxima for the quantities of interest here: hailstone size, and 10 m wind speed at hail hours. Figure 1 shows overall maximum hail sizes across each domain for each epoch. Hailstorm tracks are visible. By eye, an increase in maximum hail sizes is apparent for domains other than Perth and Brisbane, with increases in storm coverage or activity in the Adelaide, Goldfields (Kalgoorlie), Melbourne and Canberra/Sydney domains. Maximum wind speeds at hail hours are more widespread in the future scenarios than the historic scenarios, with an eastward expansion in areas experiencing maximum wind speeds in the Brisbane and Adelaide domains and a southern shift in the Goldfields (Kalgoorlie) region (Supporting Information Figure S3).
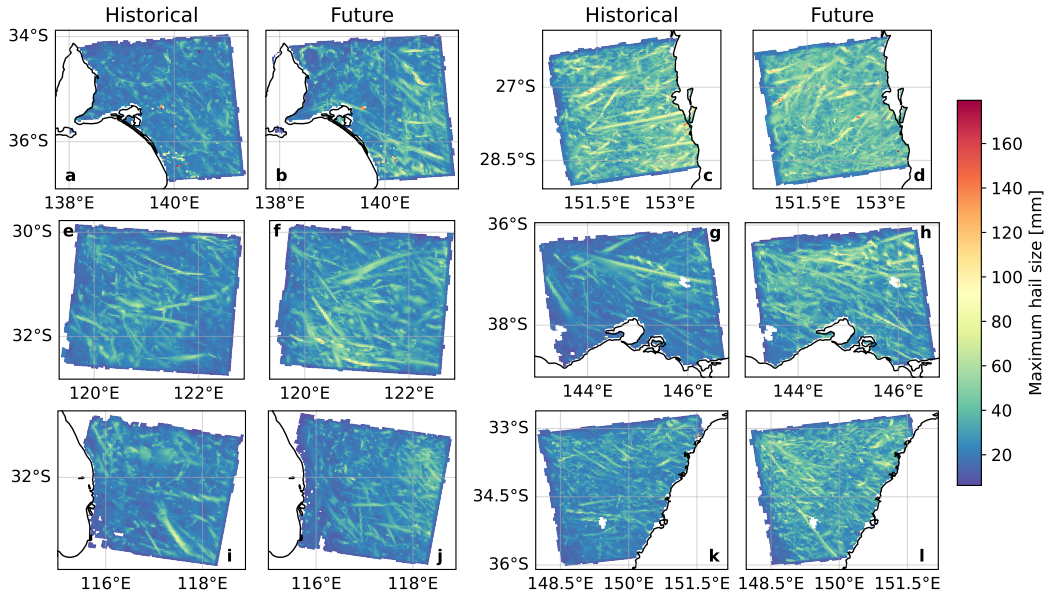

Figure 1. Maximum hail sizes in historical and future climates, for Adelaide (a, b), Brisbane (c, d), Goldfields (Kalgoorlie) (e, f), Melbourne (g, h), Perth (i, j) and Sydney/Canberra (k, l) domains. **(JA: the time period in past and future maps is not equal? 30 years vs 20 years?) (JA: − (k,l) can you plot the location of Canberra and Sydney? I feel the reviewers might comment that this domain has a boundary issue coming from the upper left corner. I don't feel that hail storms typically propagate NW to SW in this region, they typically track from the W or SW? This appears to the only domain where the behaviour of the hail storms changes in the future, if you think that is real, then we should discuss it in the text as its interesting.)**

4.2 Changes in frequency of hail

Table 1 shows changes in the frequency of hail days across the six study domains. There are significant increases in hail frequency in the Sydney/Canberra and Brisbane domains, with a 29% increase in seasonal hail days in the Sydney/Canberra region. There are small non-significant frequency decreases in Adelaide, the Goldfields (Kalgoorlie) and Melbourne domains, and an indication of an increase in seasonal hail days in the Perth region, albeit not statistically significant. The variability in seasonal hail days is similar between epochs.

Table 1. Mean and standard deviation of seasonal hail days in the historic and future simulations, and relative future changes with 95% confidence interval according to Welch's two-sample t-test, per domain. Statistical significance of the change calculated by Welch's two-sample t-test is indicated by $*$ for a 90% confidence level ($p < 0.1$) and $**$ for a 95% confidence level ($p < 0.05$).

Domain	Historic days	Future days	Future change	
Adelaide	8.7 ± 4.2	8.35 ± 4.9	-4%	(-38% to 30%)
Brisbane	32.95 ± 8.3	37.8 ± 8.8	15% $*$	(-2% to 31%)
Kalgoorlie	10 ± 6	9.8 ± 5.2	-2%	(-38% to 34%)
Melbourne	11.7 ± 5.9	11.5 ± 7.1	-2%	(-37% to 34%)
Perth	6.8 ± 4.9	7.55 ± 4.9	11%	(-35% to 57%)
Sydney/Canberra	24.3 ± 9.4	31.4 ± 9	29% $**$	(5% to 53%)

4.3 Extreme value analysis

(JA: For Sydney and Melbourne domains (or all of them) you need to plot the extreme value curves to show how the 3 parameters are changing the shape of the curves. I see the curves currently are presented after the change in the parameters. Would it be better to start with these curves rather than the change in the parameters?)

(JA: A reviewer might ask if these results are sensitive to threshold. You could also chose to keep the 3rd parameter constant if it is physically reasonable that the whole shape of the tail of the curve would not change (we force this for cyclone and flood, we do not expect the curve to increase forever with increasing RP due to physical constraints).)

4.3.1 GEV goodness of fit

GEV models were fitted to time series of daily maximum hail sizes and 10 m wind speeds at hail hours (Supporting Information Figures S4 and S5). QQ plots for hail size show acceptable agreement with some model overestimation of high quantiles (Supporting Information Figure S6), while QQ plots for wind speed at hail hours show excellent agreement between modelled and empirical quantiles (Supporting Information Figure S7). In all cases where the model was compared to empirical values, either all or the bulk of KS test p values were above the 0.05 level, indicating that the null hypothesis that the two samples are drawn from the same distribution can not be rejected (Supporting Material Figure S8). The QQ plot and KS test results show that the GEV models have sufficient goodness of fit for the analyses here.

4.3.2 Significance of changes

Having determined that the GEV fits to empirical data are valid, we now consider whether the fitted models show any significant difference between the historical and future epochs. Figure 2 shows the fitted parameters and their confidence intervals for all the GEV models used in this study. The models fitted for the Melbourne and Sydney/Canberra domains both show significant differences between epochs in the location or scale parameters for both hail size and wind at hail hours, whereas the models for the other domains have parameters with overlapping confidence intervals. These results are further supported by the p value distributions from KS tests when historical models are compared to future models (Supporting Information Figure S8). The null hypothesis that the samples are drawn from the same distribution can be rejected for the Melbourne and Sydney/Canberra domains for

both maximum hail size and maximum wind speed at hail hours, and for the Perth domain for wind only. To be conservative, we conclude that the changes in maxima between epochs are significant in the Melbourne and Sydney/Canberra domains, but not significant in the other domains.
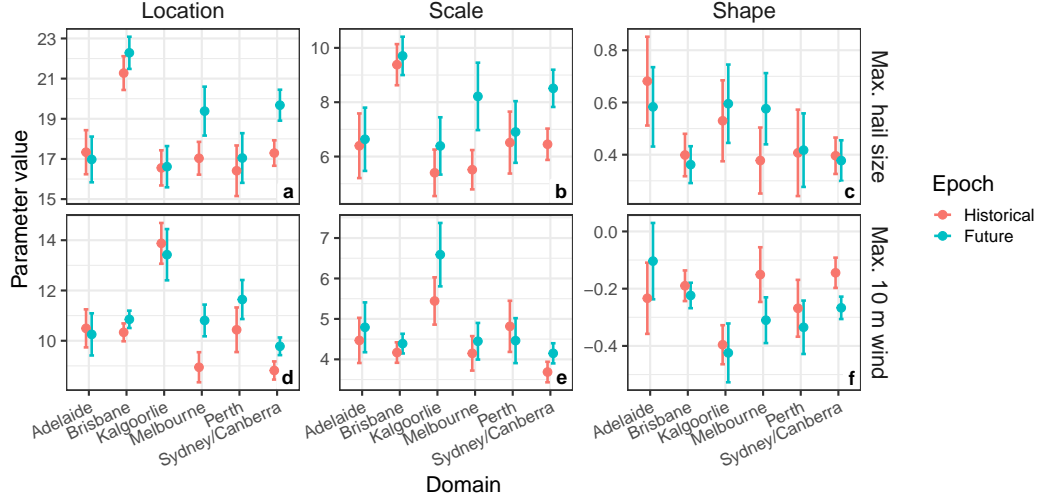

Figure 2. Location (a, d), scale (b, e), and shape (c, f) parameters for fitted GEV distributions for maximum hail size (a–c) and 10 m wind at hail hours (d–f). Parameter values are shown as a point and whiskers show 95% confidence intervals.

4.3.3 Return periods

(JA: should be showing the return period of hail days in years) (JA: Extension – can this be expanded into bivariate GEV bt wind and hail?)

Figure 3 shows return period curves for maximum hail size and maximum wind speed at hail hours. Because our analysis is limited to hail days, the return periods are in number of hail days, not overall days. It is not uncommon for return period models based on the GEV family to produce non-physical extreme values such as the extremely large hail sizes predicted for large return periods here (Coles, 2001, p. 66). We take the advice of Coles (2001) and interpret the results here based on the shorter return periods, thus keeping physical principles in mind. In Melbourne and Sydney/Canberra, the two domains with significant changes, there are increases in the maximum expected hail size for return periods longer than about three hail days, with the largest increase in the Melbourne region where the return period for 100 mm hail is reduced from more than 100 hail days to about 30 hail days. In both domains with significant changes the return period for lighter winds (less than about 18 m s^{-1}) is markedly shorter in the future scenario, but the return period for very strong winds is longer in the warmer scenario. For the other domains, with non-significant differences in GEV distributions, the most notable changes are a decrease in strong wind return periods for Adelaide and Goldfields (Kalgoorlie) regions and light wind return periods in the Perth region.

4.3.4 Probability of exceeding damaging thresholds

(JA: is hail threshold 2 cm or 5 cm? I suggest to keep repeating the threshold.)
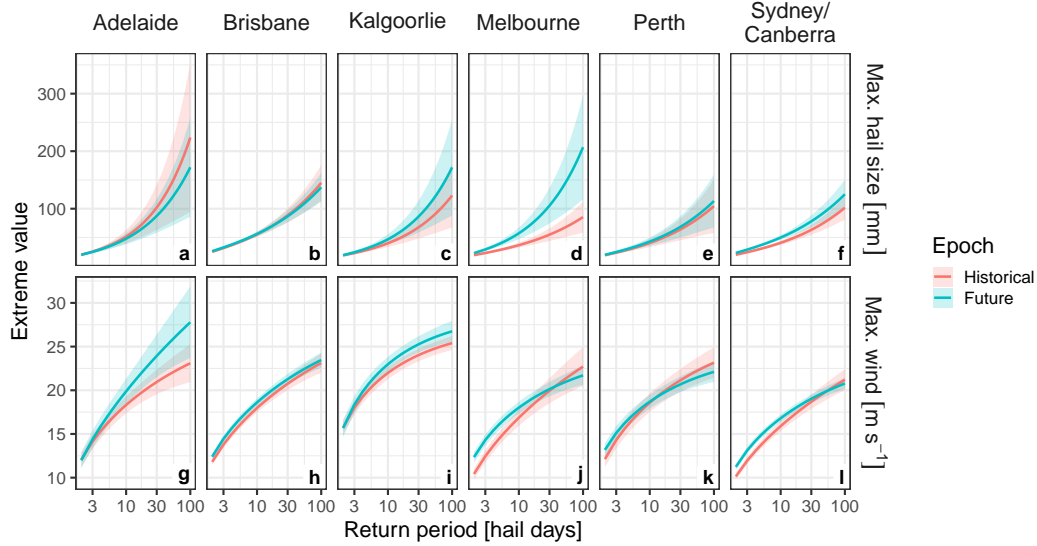
Figure 3. Return period plots for maximum hail size (a–f) and maximum wind at hail hours (g–l) for the domains of Adelaide (a, g), Brisbane (b, h), Goldfields (Kalgoorlie) (c, i), Melbourne (d, j), Perth (e, k), and Sydney/Canberra (f, l). **(JA: I find the x-axis RP unit expressed as hail days to be unusual – we want to measure if the number of days with giant hail is increasing so I think the unit has to be years Since you have extracted hail days in the season, then the measure of time is the full season.)**

Figure 4 shows the probability of a hail day producing various damaging hail and wind thresholds at hail hours (numerical results are shown in Supporting Information Table S2), comparing historical to future epochs. For hail, we examine the probability of a hail day producing severe (20 mm), giant (50 mm), and 100 mm hail, while for wind we examine 80 and 100 km h^{-1} as damaging thresholds. In the Melbourne domain for any given hail day, the probability of severe hail jumps from ∼46% in the historical epoch to ∼61% in the future scenario, while giant hail probability roughly triples (from ∼4% to ∼13%), and 100 mm hail is more than 5 times more likely (from ∼1% to ∼4%) in the future epoch. In the Sydney/Canberra domain, any given hail day has a probability of severe hail of ∼49% in the historical epoch which increases to ∼62% in the future scenario, while giant hail probability (∼6% to ∼10%) and 100 mm hail probability (∼1% to ∼2%) both come close to doubling in the future epoch. Other non-significant increases in severe hail probability are shown for Brisbane, Perth, and Goldfields (Kalgoorlie) areas, with non-significant decreases in the Adelaide region, and the Goldfields region shows a non-significant increase also for giant hail probability. In Melbourne and Sydney/Canberra, the domains with significant differences, the probability of damaging winds at hail hours on a hail day decreases by about half for 80 km h^{-1} wind speed at hail hours. Non-significant changes include an increase in the probability of 80 km h^{-1} wind speed at hail hours in the Goldfields (Kalgoorlie) region (from ∼9% to ∼13%) and Adelaide domain (from ∼2% to ∼5%), and for 100 km h^{-1} winds at hail hours for the Adelaide region (from ∼0% to ∼1%). Other than for Adelaide, the probability of hail days producing 100 km h^{-1} wind speed at hail hours is close to zero in all domains across both epochs.
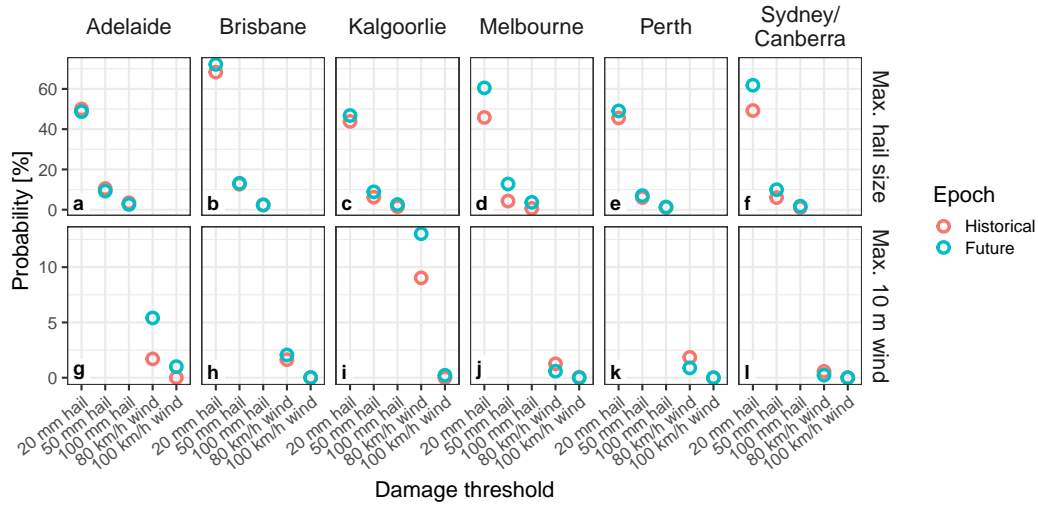
Figure 4. Changes in the probability of exceeding thresholds on hail size (a–f), and 10 m wind speed at hail hours (g–l), on any given hail day, for the domains of Adelaide (a, g), Brisbane (b, h), Goldfields (Kalgoorlie) (c, i), Melbourne (d, j), Perth (e, k), and Sydney/Canberra (f, l). **(JA: can the significant results have filled in circles?)**

4.4 Changes in relevant atmospheric properties

Table 2 shows projected changes in daily mean hail size, wind speed, and storm-relevant atmospheric properties, at hail times, in the future compared to historical simulations. Unlike in the extreme value analysis above, here we used mean values for each season and test for differences between epochs using Welch's t-test. Mean hail size shows statistically significant increases **(JA: quantify increase here)** in Melbourne and Sydney/Canberra, aligning with the extreme value analysis results for maximum hail size, but here there is also a significant increase in the Brisbane domain. Changes in mean wind are generally small, with the only significant changes being increases in the Perth and Sydney/Canberra domains. Changes in wind shear are varied, with a small significant increase in Kalgoorlie and a small significant decrease in Brisbane. Increases of ~1% in temperature at 500 hPa, and 8-10% in freezing-level and melting-level heights are significant in every domain. Atmospheric instability increases in all domains, with significant increases in convective available potential energy (CAPE) at hail times in Adelaide, Brisbane, Melbourne, and Sydney/Canberra regions, while the results for lifted index (LI) are more mixed with fewer significant changes. Convective inhibition (CIN) also became stronger in all domains with significant decreases in Adelaide, Brisbane, the Goldfields (Kalgoorlie), Melbourne, and Sydney/Canberra. Lapse rate changes are generally small, although significant increases are shown in Brisbane and Sydney/Canberra. The extreme value analysis results for the domains where they showed significant changes, Melbourne and Sydney/Canberra, are supported by the large increases in convective instability and convective inhibition and freezing level height, that would support storm development, strong updrafts, and survival of large hailstones to the surface. Wind shear changes are not significant, indicating that these changes in damage are driven more by changes in instability than shear. In the Brisbane domain there is more of a balance between modest yet significant increases in instability and decreases in wind shear, indicating that in this domain there may be more offsetting of these two environmental factors leading to no significant change in damage potential in the GEV analyses.

Table 2. Projected relative changes in mean hail size, 10 m wind (Wind), bulk vertical wind shear from 0-6 km (S06), convective available potential energy (CAPE), convective inhibition (CIN), lifted index (LI), temperature at 500 hPa (T500), lapse rate from 700 to 500 hPa (LR), freezing-level height (FLH), and melting-level height (MLH), for hail times by domain. Statistical significance of the difference between historical and future seasonal mean values, calculated using Welch's two-sample t-test, is shown by ∗ for the 90% confidence level, ∗∗ for the 95% confidence level, and ∗∗∗ for the 99% confidence level. Bracketed ranges show the 95% confidence interval on the changes. Means are daily means of variables at hail times and locations. **(JA: need to emphasise these stats are over the domain. Is there a threshold hail size here? In Fig 1, Melbourne seems to have more extensive 8cm + hail but this is not coming out in trends.)**

	Adelaide		Brisbane		Kalgoorlie	
Hail size	0%	(-4% to 3%)	4%∗∗∗	(2% to 5%)	0%	(-3% to 4%)
Wind	-1%	(-7% to 5%)	2%	(-1% to 4%)	-2%	(-7% to 3%)
S06	-1%	(-9% to 7%)	-4%∗∗	(-7% to 0%)	5%∗	(-1% to 11%)
CAPE	23%∗	(-2% to 49%)	9%∗∗	(2% to 15%)	11%	(-8% to 29%)
LI	-41%	(-146% to 65%)	-8%∗∗	(-16% to 0%)	77%∗	(-7% to 161%)
CIN	-22%∗∗	(-40% to -4%)	-8%∗∗∗	(-14% to -2%)	-13%∗∗	(-25% to -1%)
LR	-1%	(-3% to 1%)	2%∗∗∗	(1% to 3%)	-1%	(-2% to 1%)
T500	1%∗∗∗	(1% to 1%)	1%∗∗∗	(1% to 1%)	1%∗∗∗	(1% to 1%)
FLH	9%∗∗∗	(7% to 11%)	9%∗∗∗	(8% to 10%)	9%∗∗∗	(6% to 11%)
MLH	8%∗∗∗	(6% to 10%)	9%∗∗∗	(8% to 10%)	9%∗∗∗	(6% to 11%)

	Melbourne		Perth		Sydney/Canberra	
Hail size	4%∗∗	(1% to 7%)	1%	(-3% to 6%)	4%∗∗∗	(2% to 6%)
Wind	3%	(-2% to 8%)	9%∗∗∗	(3% to 15%)	3%∗	(0% to 6%)
S06	6%	(-2% to 13%)	-2%	(-10% to 6%)	-1%	(-6% to 3%)
CAPE	29%∗∗∗	(14% to 44%)	14%	(-11% to 38%)	25%∗∗∗	(16% to 34%)
LI	-13%	(-77% to 50%)	12%	(-72% to 96%)	-21%	(-48% to 6%)
CIN	-23%∗∗∗	(-36% to -10%)	-7%	(-21% to 6%)	-15%∗∗∗	(-23% to -7%)
LR	1%	(0% to 3%)	1%	(-2% to 3%)	2%∗∗∗	(1% to 3%)
T500	1%∗∗∗	(1% to 1%)	1%∗∗∗	(0% to 1%)	1%∗∗∗	(1% to 1%)
FLH	10%∗∗∗	(8% to 12%)	8%∗∗∗	(4% to 11%)	9%∗∗∗	(8% to 10%)
MLH	10%∗∗∗	(8% to 12%)	7%∗∗∗	(4% to 10%)	9%∗∗∗	(7% to 10%)

4.5 Correlations between regions

Correlations between seasonal values of hail relevant properties are shown in Figure 5. There is co-fluctuation in hail days between the east-coast cities of Melbourne, Sydney/Canberra and Brisbane in both historical and future epochs, with Adelaide significantly correlated with Melbourne and Sydney/Canberra in the future projections. Correlations in hail diameter between the domains around Kalgoorlie, Perth, Melbourne, and Sydney/Canberra are considerably stronger in the future projections that in the historical epoch, while wind correlations between the Perth region and other south-western domains of Adelaide and Kalgoorlie are evident in the historical epoch but disappear in the future projections. Instability is correlated between Melbourne and Sydney/Canberra domains in both epochs. Temperature-related parameters show strong correlations between nearby domains, such as the western domains of the Goldfields (Kalgoorlie) and Perth, which increase in strength in the projections, and the eastern domains of Brisbane and Sydney/Canberra.
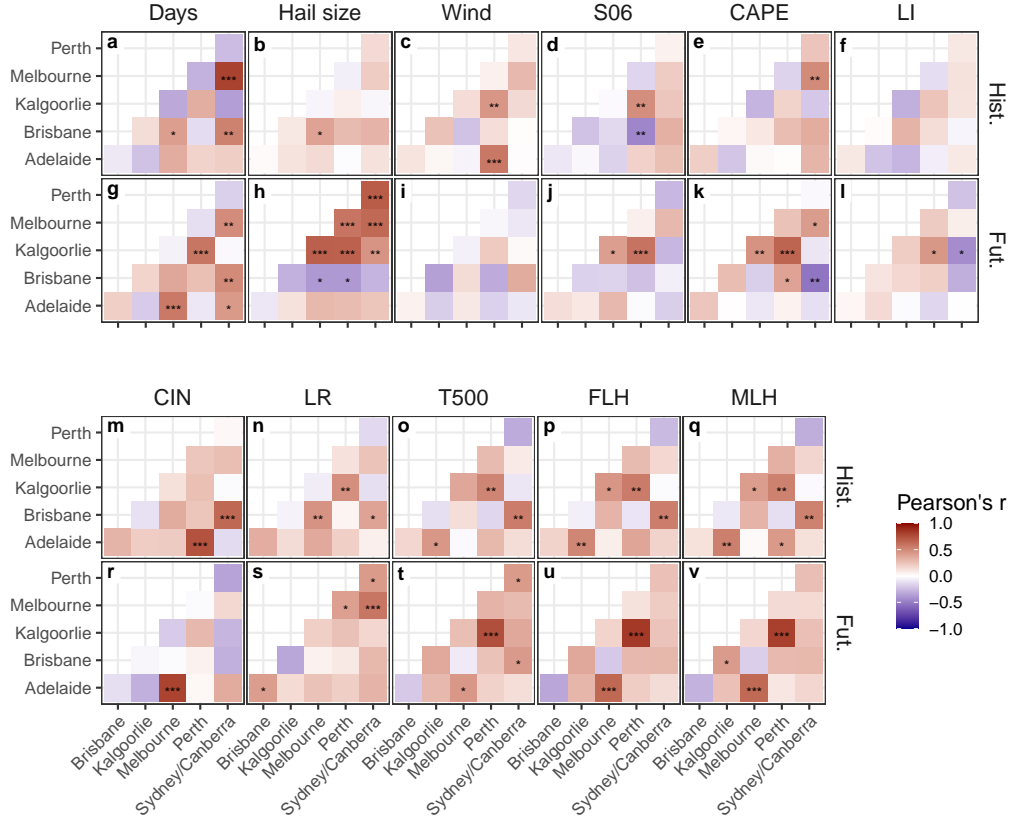
Figure 5. Correlations of seasonal values of hail-relevant properties between domains, by epoch. Seasonal means were calculated from daily means at hail locations and hours. Variables considered are seasonal hail days (a, g), and mean hail diameter (b, h), 10 m wind at hail hours (c, i), bulk vertical wind shear (d, j), CAPE (e, k), lifted index (f, l), CIN (m, r), 700-500 hPa lapse rate (n, s), temperature at 500 hPa (o, t), freezing level height (p, u) and melting level height (q, v), for historical (a-f, m-q) and future (g-l, r-v) epochs. Statistically significant correlations are shown by an ∗ for 90% confidence level ($p < 0.1$), ∗∗ for 95% confidence level ($p < 0.05$), and ∗∗∗ for the 99% confidence level ($p < 0.01$).

5 Conclusions

In this study we used downscaled regional analyses to project changes in hail diameter and coincident wind speeds in warmer conditions, over hail-prone regions of Australia. The climate scenario considered was for SSP2-4.5 for the period 2080–2099 compared to a 1989–2019 baseline, using **(eight)** CMIP ensemble members. The domains covered more than 60% of Australia's population, including the major cities of Perth, Adelaide, Melbourne, Canberra, Sydney, and Brisbane. The results show projected increases in hail frequency around Sydney/Canberra and Brisbane, projected increases in hail size around Sydney/Canberra and Melbourne, and indications of increased wind at hail hours in Adelaide and the remote Goldfields region but decreased probability of damaging wind at hail hours in Melbourne, Perth, and Sydney/Canberra. An analysis of the changes in mean atmospheric conditions at hail hours shows projected increases in atmospheric instability and freezing level height, and little change in bulk vertical wind shear in the warmer scenario. Correlations in seasonal

average hail size between regions are stronger in the future than present scenario. **(JA: Conclusion – add quantification)**

(Relate changes to similar studies, eg for wind.)

Several caveats apply to the results shown here. The most notable is that maximum hail sizes reported at each hour are maximums over the last hour, while wind speeds are instantaneous values within the temporal vicinity of hail occurrence. Maximum wind gusts over the previous hour would generally be significantly stronger than these instantaneous values. We also caution that these results are one realization of possible future projections, based on the boundary conditions and modelling framework used, and more ensemble members using different setups are required to build a more complete picture of possible future hazards.

(JA: Note on storm season – 2 of our top 20 hail events occurred in Autumn - Rockhampton hail storm April 2020 and Gosford hail May 2023 (and the 1999 Sydney hail storm occurred in April too))

(JA: future work, applicability to insurance industry and building code, impact of correlation bt regions on insurance and building recovery. See paragraph at end of this document.)

(JA's text:) This study shows that the frequency and severity of damaging hail events may increase in major population centres of Australia in a warming climate. This poses an increasing risk to communities in terms of personal safety and through building damage, solar panel damage, water ingress and damage to interiors, contents and cars and loss of use of commercial, civil and residential buildings for extended periods. The damage from giant hail events can be extreme causing extensive structural damage and complete loss of amenity of a building and widespread community disruption as seen in the 2020 Halloween hailstorm in southeastern Queensland. The increasing correlation of hail events in multiple cities poses a challenge to community resilience for the increased resources required for rebuilding efforts. For insurers, storm losses account for a quarter of all Australian natural catastrophe losses (Insurance Council of Australia, 2024) and this is likely to increase in the future as giant hail events increase in key centres, which may result in higher insurance premiums and reinsurance costs.

These projections could be incorporated into the Australian building code, which as mentioned in the Introduction does not consider hail loading, to strengthen the resilience of buildings in the face of a changing climate.

Future work in this area may include consideration of the win-driven hail processes and how they may change with climate change at higher resolution, extension to other countries such as New Zealand and extension to a wider range of climate scenarios and timeframes.

Open Research Section

Boundary condition data are available at Xu et al. (2021a). Complete analysis code and WRF configuration files are available in a **(Zenodo repository)**. Convective parameters were calculated using `xarray_parcel` (DOI: 10.5281/zenodo.8088497).

Acknowledgments

the Australian Government. We thank Simon Tett for useful discussions on extreme value
techniques.

References

Adams-Selin, R. D., Clark, A. J., Melick, C. J., Dembek, S. R., Jirak, I. L., & Ziegler, C. L. (2019). Evolution of WRF-HAILCAST during the 2014–16 NOAA/Hazardous Weather Testbed spring forecasting experiments. *Weather Forecast*, *34*(1), 61-79. doi: 10.1175/waf-d-18-0024.1

Allen, J. T. (2018, 07). *Climate change and severe thunderstorms.* Oxford University Press. doi: 10.1093/acrefore/9780190228620.013.62

Allen, J. T., Karoly, D. J., & Walsh, K. J. (2014). Future Australian severe thunderstorm environments. Part II: The influence of a strongly warming climate on convective environments. *J Climate*, *27*(10), 3848-3868. doi: 10.1175/JCLI-D-13-00426.1

Association of Consulting Structural Engineers. (2022). *Hail loading on roofs. Practice note number 19 version 2.* Retrieved from https://www.acse.org.au/wp-content/uploads/2022/03/Practice-Paper-19-Hail-Loading-REVISED-2022.pdf (accessed 22 June 2024)

Australian Building Codes Board. (2024). *National construction code.* Retrieved from https://ncc.abcb.gov.au (accessed 22 July 2024)

Australian Bureau of Meteorology. (2021). *Bureau expert explains giant hail phenomenon.* Retrieved from https://media.bom.gov.au/releases/908/bureau-expert-explains-giant-hail-phenomenon/ (Media release, accessed 31 July 2023)

Bell, J. R., Wisinski, E. F., Molthan, A. L., Schultz, C. J., Gilligan, E., & Sharp, K. G. (2023). Developing a hail and wind damage swath event database from daily MODIS true color imagery and storm reports for impact analysis and applications. *Weather Forecast*, *38*(9), 1575 - 1588. doi: 10.1175/WAF-D-22-0210.1

Brimelow, J. C., Reuter, G. W., & Poolman, E. R. (2002). Modeling maximum hail size in Alberta thunderstorms. *Weather Forecast*, *17*(5), 1048-1062. doi: 10.1175/1520-0434(2002)017⟨1048:MMHSIA⟩2.0.CO;2

Brown, A., & Dowdy, A. (2021). Severe convective wind environments and future projected changes in Australia. *J Geophys Res-Atmos*, *126*(16), e2021JD034633. (e2021JD034633 2021JD034633) doi: 10.1029/2021JD034633

Carletta, N. D. (2010). *Severe wind-driven hail events: Dependence on convective morphology and larger-scale environment* (Master's thesis, Department of Geological and Atmospheric Sciences. Iowa State University). Retrieved from https://meteor.geol.iastate.edu/~ncarlett/portfolio/Senior_Thesis_Carletta_Final.pdf (accessed 22 July 2024)

Changnon, S. A. (1967). Areal-temporal variations of hail intensity in Illinois. *J Appl Meteorol*, *6*(3), 536 - 541. doi: 10.1175/1520-0450(1967)006⟨0536:ATVOHI⟩2.0.CO;2

Coles, S. (2001). *An introduction to statistical modeling of extreme values* (1st ed.). Springer London. doi: 10.1007/978-1-4471-3675-0

Eccel, E., Cau, P., Riemann-Campe, K., & Biasioli, F. (2012). Quantitative hail monitoring in an alpine area: 35-year climatology and links with atmospheric variables. *Int J Climatol*, *32*(4), 503-517. doi: 10.1002/joc.2291

Eyring, V., Bony, S., Meehl, G. A., Senior, C. A., Stevens, B., Stouffer, R. J., & Taylor, K. E. (2016). Overview of the Coupled Model Intercomparison Project Phase 6 (CMIP6) experimental design and organization. *Geosci Model Dev*, *9*(5), 1937–1958. doi: 10.5194/gmd-9-1937-2016

Gilleland, E., & Katz, R. W. (2016). extRemes 2.0: An extreme value analysis package in R. *J Stat Softw*, *72*(8), 1–39. doi: 10.18637/jss.v072.i08

Gutiérrez, J., Jones, R., Narisma, G., Alves, L., Amjad, M., Gorodetskaya, I., ... Yoon, J.-H. (2021). Atlas. In V. Masson-Delmotte et al. (Eds.), *Climate change 2021: The physical science basis. Contribution of working group I to the Sixth Assessment*

Report of the Intergovernmental Panel on Climate Change (p. 1927–2058). Cambridge, United Kingdom and New York, NY, USA: Cambridge University Press. doi: 10.1017/9781009157896.021

Hersbach, H., Bell, B., Berrisford, P., Hirahara, S., Horányi, A., Muñoz Sabater, J., . . . Thépaut, J.-N. (2020). The ERA5 global reanalysis. *Q J Roy Meteor Soc*, *146*(730), 1999-2049. doi: 10.1002/qj.3803

Hong, S.-Y., Noh, Y., & Dudhia, J. (2006). A new vertical diffusion package with an explicit treatment of entrainment processes. *Mon Weather Rev*, *134*(9), 2318 - 2341. doi: 10.1175/MWR3199.1

Iacono, M. J., Delamere, J. S., Mlawer, E. J., Shephard, M. W., Clough, S. A., & Collins, W. D. (2008). Radiative forcing by long-lived greenhouse gases: Calculations with the AER radiative transfer models. *J Geophys Res-Atmos*, *113*(D13). doi: 10.1029/2008JD009944

Institute for Catastrophic Loss Reduction. (2018). *Protect your home from hail.* Retrieved from https://www.iclr.org/wp-content/uploads/2021/04/ICLR_Hail-2020_E_2021.pdf (accessed 22 July 2024)

Insurance Council of Australia. (2024). *Historical normalised catastrophes, June 2024.* Retrieved from https://insurancecouncil.com.au/wp-content/uploads/2024/07/ICA-Historical-Normalised-Catastrophe-June-2024.xlsx (accessed 22 July 2024)

International Code Council. (2008). *International building code - structural.* Retrieved from https://www.iccsafe.org/cs/codes/Documents/2007-08cycle/FAA/IBC-S1-S141-P2.pdf (accessed 22 July 2024)

Jiménez, P. A., Dudhia, J., González-Rouco, J. F., Navarro, J., Montávez, J. P., & García-Bustamante, E. (2012). A revised scheme for the WRF surface layer formulation. *Mon Weather Rev*, *140*(3), 898 - 918. doi: 10.1175/MWR-D-11-00056.1

Milbrandt, J. A., Morrison, H., II, D. T. D., & Paukert, M. (2021). A triple-moment representation of ice in the predicted particle properties (P3) microphysics scheme. *J Atmos Sci*, *78*(2), 439 - 458. doi: 10.1175/JAS-D-20-0084.1

Niu, G.-Y., Yang, Z.-L., Mitchell, K. E., Chen, F., Ek, M. B., Barlage, M., . . . Xia, Y. (2011). The community Noah land surface model with multiparameterization options (Noah-MP): 1. Model description and evaluation with local-scale measurements. *J Geophys Res-Atmos*, *116*(D12). doi: 10.1029/2010JD015139

O'Neill, B. C., Kriegler, E., Ebi, K. L., Kemp-Benedict, E., Riahi, K., Rothman, D. S., . . . Solecki, W. (2017). The roads ahead: Narratives for shared socioeconomic pathways describing world futures in the 21st century. *Glob Environ Change*, *42*, 169-180. doi: 10.1016/j.gloenvcha.2015.01.004

R Core Team. (2023). R: A language and environment for statistical computing [Computer software manual]. Vienna, Austria. Retrieved from https://www.R-project.org/

Raupach, T. H., Martius, O., Allen, J. T., Kunz, M., Lasher-Trapp, S., Mohr, S., . . . Zhang, Q. (2021). The effects of climate change on hailstorms. *Nat Rev Earth Environ*, *2*(3), 213-226. doi: 10.1038/s43017-020-00133-9

Raupach, T. H., Soderholm, J., Protat, A., & Sherwood, S. C. (2023). An improved instability–shear hail proxy for australia. *Mon Weather Rev*, *151*(2), 545-567. doi: 10.1175/MWR-D-22-0127.1

Raupach, T. H., Soderholm, J. S., Warren, R. A., & Sherwood, S. C. (2023). Changes in hail hazard across Australia: 1979-2021. *npj Clim Atmos Sci*, *6*(1), 143. doi: 10.1038/s41612-023-00454-8

Skamarock, W. C., Klemp, J. B., Dudhia, J., Gill, D. O., Liu, Z., Berner, J., . . . yu Huang, X. (2021, 7 20). *A description of the advanced research WRF version 4.3* (Tech. Rep.). Boulder, Colorado, USA: National Center for Atmospheric Research. (NCAR technical note NCAR/TN-556+STR) doi: 10.5065/1dfh-6p97

Standards Australia. (2021). *AS/NZS 1170.2 structural design actions, part 2 wind actions.* Retrieved from https://store.standards.org.au/product/as-nzs-1170-2-2021 (accessed 22 July 2024)

Towery, N. G., Morgan, G. M., & Changnon, S. A. (1976). Examples of the wind factor in crop-hail damage. *J Appl Meteorol*, *15*(10), 1116 - 1120. doi: 10.1175/1520-0450(1976) 015⟨1116:EOTWFI⟩2.0.CO;2

Walsh, K., White, C. J., McInnes, K., Holmes, J., Schuster, S., Richter, H., ... Warren, R. A. (2016). Natural hazards in Australia: storms, wind and hail. *Climatic Change*, *139*(1), 55-67. doi: 10.1007/s10584-016-1737-7

Xu, Z., Han, Y., Tam, C.-Y., Yang, Z.-L., & Fu, C. (2021a, January). *Bias-corrected CMIP6 global dataset for dynamical downscaling of the Earth's historical and future climate (1979-2100)*. Science Data Bank. doi: 10.11922/sciencedb.00487

Xu, Z., Han, Y., Tam, C.-Y., Yang, Z.-L., & Fu, C. (2021b). Bias-corrected CMIP6 global dataset for dynamical downscaling of the historical and future climate (1979–2100). *Sci Data*, *8*(1), 293. doi: 10.1038/s41597-021-01079-3

Zhang, C., & Wang, Y. (2017). Projected future changes of tropical cyclone activity over the Western North and South Pacific in a 20-km-mesh regional climate model. *J Climate*, *30*(15), 5923 - 5941. doi: 10.1175/JCLI-D-16-0597.1